Acta Crystallographica Section B
Structural Science
ISSN 0108-7681

Redetermination of the structure and dielectric properties of bis(thiourea) pyridinium iodide – a new ferroelectric inclusion compound

H. Małuszyńska, P. Czarnecki,* Z. Fojud and J. Wąsicki

Faculty of Physics, A. Mickiewicz University, Umultowska 85, 61-614 Poznań, Poland

Correspondence e-mail: pczarnec@amu.edu.pl

Received 20 September 2007
Accepted 16 June 2008

The crystal structure of bis(thiourea) pyridinium iodide (T_2PyI) was previously determined at 295 and 110 K [Prout, Heyes, Dobson, McDaid, Maris, Mueller & Seaman (2000). *Chem. Mater.* **12**, 3561–3569] and the two phases were described in the space groups *Cmcm* and $P2_1cn$, respectively. Because differential scanning calorimetry revealed two phase transitions, at 161 and 141 K, a redetermination of the structure of T_2pyI at 295, 155 and 110 K has been undertaken, and the following sequence of space groups obtained: *Cmcm* (I) $\rightarrow$ *C*2*cm* (II) $\rightarrow$ $P2_1cn$ (III). The high- (I) and low-temperature (III) phases confirmed the results reported in the previous study. In the new intermediate phase II, the mirror plane perpendicular to the *x* axis vanishes and the crystal structure loses the centre of symmetry. In phases I and II the pyridinium cations are strongly dynamically disordered, while in the low-temperature phase III the cations are well ordered. In all three phases the thiourea–iodine hydrogen-bonded sublattice is very well ordered. Dielectric measurements show that the intermediate and low-temperature phases are ferroelectric and that 161 K is the Curie point of a new ferroelectric crystal.

1. Introduction

Ferroelectricity is an important physico-chemical property of matter. Ferroelectric materials have been widely applied, for example, in nanodevices (Scott, 2000) and in random access memory (RAM). Materials showing ferroelectric properties at room temperature are of special interest because they can offer greater possibilities for use in such applications.

Recently, ferroelectric properties have been discovered in a number of pyridinium salts belonging to a new family of molecular–ionic crystals (Czarnecki *et al.*, 1994*a*,*b*; Wąsicki *et al.*, 1997; Pająk *et al.*, 1998, 2000; Małuszyńska & Czarnecki, 2006). These pyridinium complexes undergo one (salts of type I) or two or more (salts of type II) reversible phase transitions. In type I pyridinium salts, with simple anions such as I^-, Cl^- and Br^-, the phase transitions are related only to the reorientational behaviour of the heteroaromatic pyridinium rings, and these salts exhibit no ferroelectric properties. In type II salts, with polyatomic anions such as BF_4^-, ClO_4^-, ReO_4^-, IO_4^-, FSO_3^- and $FCrO_3^-$, in addition to the reorientational behaviour of the pyridinium cation, the ordering of the tetrahedral anions induces phase transitions and some of the phases are ferroelectric (Czarnecki *et al.*, 1994*a*,*b*; Pająk *et al.*, 1998, 2000, 2002). The crystals of type II pyridinium salts exhibit translational order and dynamic orientational disorder of ions, which in the low-temperature phase can be continuously or discontinuously transformed into orientational order. The nature of the ferroelectricity is connected with ordering of the

Table 1
Crystal data and structure refinement for T_2PyI at 295, 155 and 110 K.

	I	II	III
Crystal data			
Chemical formula	$CS(NH_2)_2{\cdot}C_5H_6N^+{\cdot}I^-$	$CS(NH_2)_2{\cdot}C_5H_6N^+{\cdot}I^-$	$CS(NH_2)_2{\cdot}C_5H_6N^+{\cdot}I^-$
M_r	359.25	359.25	359.25
Cell setting, space group	Orthorhombic, *Cmcm*	Orthorhombic, *C2cm*	Orthorhombic, $P2_1cn$
Temperature (K)	295.0 (2)	155.0 (2)	110.0 (2)
a, b, c (Å)	15.180 (3), 11.827 (2), 8.375 (2)	15.022 (3), 11.227 (2), 8.341 (2)	14.860 (1), 11.291 (1), 8.307 (2)
V (Å^3)	1503.6 (5)	1406.7 (5)	1393.8 (4)
Z	4	4	4
D_x (Mg m^{-3})	1.587	1.696	1.712
Radiation type	Mo $K\alpha$	Mo $K\alpha$	Mo $K\alpha$
μ (mm^{-1})	2.39	2.55	2.58
Crystal form, colour	Needle, colourless	Needle, colourless	Needle, colourless
Crystal size (mm)	0.6 × 0.1 × 0.1	0.6 × 0.1 × 0.1	0.6 × 0.1 × 0.1
Data collection			
Diffractometer	Kuma KM-4	Kuma KM-4	Kuma KM-4
Data collection method	ω–2θ	ω–2θ	ω–2θ
Absorption correction	φ scan	φ scan	φ scan
T_{min}	0.51	0.55	0.539
T_{max}	0.56	0.62	0.596
No. of measured, independent and observed reflections	2244, 1158, 965	1960, 1010, 920	4104, 2116, 1223
Criterion for observed reflections	$I > 2\sigma(I)$	$I > 2\sigma(I)$	$I > 2\sigma(I)$
R_{int}	0.024	0.027	0.036
θ_{max} (°)	30.0	30.1	30.1
No. and frequency of standard reflections	2 every 100 reflections	2 every 100 reflections	2 every 100 reflections
Refinement			
Refinement on	F^2	F^2	F^2
$R[F^2 > 2\sigma(F^2)]$, $wR(F^2)$, S	0.029, 0.090, 0.74	0.022, 0.058, 1.01	0.027, 0.075, 0.99
No. of reflections	1158	1010	2116
No. of parameters	50	104	137
No. of restraints	0	1	1
H-atom treatment	Constrained†	Constrained†	Constrained†
Weighting scheme	$w = 1/[\sigma^2(F_o^2) + (0.1P)^2]$ where $P = (F_o^2 + 2F_c^2)/3$	$w = 1/[\sigma^2(F_o^2) + (0.0422P)^2]$ where $P = (F_o^2 + 2F_c^2)/3$	$w = 1/[\sigma^2(F_o^2) + (0.0417P)^2]$ where $P = (F_o^2 + 2F_c^2)/3$
$(\Delta/\sigma)_{max}$	0.135	0.148	0.001
$\Delta\rho_{max}$, $\Delta\rho_{min}$ (e Å^{-3})	0.67, −0.91	0.76, −0.69	2.14, −1.10
Absolute structure	–	Flack (1983)	Flack (1983)
Flack parameter	–	0.35 (10)	0.46 (7)

Computer programs used: *KM-4 Software* (Kuma Diffraction, 1999), *SHELXS97* and *SHELXL97* (Sheldrick, 2008). † Constrained to parent site.

dipole moments of pyridinium cations and/or with distortion of tetrahedral anions, which results in the appearance of an additional dipole moment of the anion.

Thiourea is a well known molecule, which forms inclusion complexes with various organic molecules. In these complexes, thiourea molecules, being the hosts, form hexagonal channels in which the organic molecules, the guests, are located (Harris, 1996; Hollingsworth & Harris, 1996). Thiourea pyridinium halide crystals were investigated first by Truter & Vickery (1972) and later by Prout *et al.* (2000). In these crystal structures, thiourea molecules form square cross-sectional channels of hydrogen-bonded thiourea molecules in which dynamically disordered pyridinium cations are situated. The halide ions (I^-, Br^- or Cl^-) are located at the apex of the cross section of the channel. It has been reported previously (Prout *et al.*, 2000) that only the bromide derivative undergoes two phase transitions, while in the two remaining compounds only one phase transition has been reported with no phase transition temperatures given.

Using differential scanning calorimetry (DSC), X-ray diffraction and dielectric spectroscopy we have determined two, instead of one, phase transitions in bis(thiourea) pyridinium iodide (hereafter T_2PyI). We have resolved the crystal and molecular structures of all three polymorphs, and, in what seems to be the most important finding, we have discovered a new ferroelectric phase below 161 K.

2. Experimental

DSC measurements were carried out using a TA Instruments Q2000 system. The complex calibration of the DSC apparatus was used for heat capacity measurements, using a sapphire disc and an indium sample. The heating/cooling rate was 10 K min^{-1} and the weight of the T_2PyI powder sample was 7.98 mg.

For the X-ray single-crystal diffraction, a transparent needle-like crystal of size 0.1 × 0.1 × 0.6 mm coated in paraffin oil was mounted on a Kuma KM-4 diffractometer. Intensity data were collected with the ω–2θ technique, using

Mo $K\alpha$ graphite-monochromated radiation (λ = 0.71073 Å). Cell dimensions were obtained from the setting angles of 34 reflections in the 2θ range 14–25°. Lorenz polarization and semi-empirical absorption corrections were applied. The temperature measurements were performed using an Oxford Cryostream liquid nitrogen cooler with an accuracy of ±0.2 K.

The structure was solved by direct methods using *SHELXS*97 and refined by the full-matrix least-squares method on F^2 with *SHELXL*97 (Sheldrick, 2008). The H-atom positions in the thiourea molecules and ordered pyridinium cation were obtained from a difference-Fourier map and allowed to ride with appropriate isotropic displacement parameters and normalized C—H and N—H distances of 1.08 and 1.03 Å, respectively. Crystallographic data and structure refinement details for the three phases are given in Table 1.[1]

The dielectric properties were studied in pressed polycrystalline pellets with silver electrodes deposited on the surfaces. The complex permittivity was measured by an impedance analyser (Hewlett-Packard 4192 A) at frequencies between 10 kHz and 13 MHz. The hysteresis loop was measured with a Diamant–Drenck–Pepinsky bridge (Radiopan MD 2/1) at a frequency of 50 Hz on the same pellets as used for permittivity measurements.

3. Discussion

3.1. Differential scanning calorimetry

The specific heat values, C_p, determined by DSC are presented in Fig. 1. The anomalies in the temperature dependence of the specific heat clearly indicate the occurrence of two phase transitions in T_2PyI, one at T_1 = 161 K and another at T_2 = 141 K, in contrast to the result of Prout *et al.* (2000), who reported only one phase transition and did not specify its temperature.

The characters of the specific heat anomalies at T_1 and T_2 are different. Below T_1 the temperature dependence of the specific heat decreases in the form of a long tail, suggesting pre-critical effects preceding this transition. The lack of a distinct peak of the specific heat at the phase transition temperature T_1, the lack of thermal hysteresis and a jumpwise change in C_p at T_1 imply a continuous phase transition at T_1. In contrast, at the second phase transition temperature T_2, there is a distinct peak of the specific heat, which suggests a discontinuous phase transition. However, the small thermal hysteresis on heating and cooling, of $\sim$ 0.3 K, and a small tail on the low-temperature side indicate that the transition, although discontinuous, is close to continuous.

3.2. X-ray structure of T_2PyI at 295, 155 and 110 K

The crystal structures of the high-temperature phase I and the low-temperature phase III confirm the results reported by Prout *et al.* (2000). The newly discovered intermediate phase II belongs to the orthorhombic system and crystallizes in the noncentrosymmetric space group *C*2*mc* (whose standard setting is *Ama*2, No. 40). Therefore, the correct sequence of phases in T_2PyI is *Cmcm* (I) → *C*2*cm* (II) → *P*2$_1$*cn* (III). In all three phases the hydrogen-bonded thiourea molecules, together with the iodide anions, form ribbons. Four of these ribbons form square cross-sectional channels running along the *z* axis. In these channels, formed within the host sublattice, are located pyridinium cations, the guest molecules. Only the position and orientation of the pyridinium cations within the channel, together with their dynamics, differentiate these three crystal phases.

In the high-temperature phase I, the asymmetric unit contains half of the thiourea molecule, one-quarter of the pyridinium cation and one-quarter of the iodide ion. The thiourea molecules are well ordered. The pyridinium cation is located at the 2/*m* symmetry site and the hexagonal ring is described by three independent atoms: atoms C2 and C3 lying in general positions and atom C1 on the mirror plane. The N-atom position could not be localized and refinement with a variable occupancy factor of the N atom did not improve the model of the cation. This model indicates not only rotational cationic disorder but also suggests a wobbling of the pyridinium ring around an axis running through C1 and C1*A*, with a wobbling angle of around 33°.

The second-order phase transition at 161 K transforms the crystal structure into the noncentrosymmetric space group *C*2*cm*, in which the mirror plane *m* perpendicular to the *x* axis vanishes and the phase loses the centre of symmetry. The asymmetric unit contains two half thiourea molecules, half of the pyridinium cation and half of the iodide ion. The pyridinium cation is located at the 2 symmetry site and is described by six C atoms in general positions (since the N atoms could not be localized), giving 12 C atoms with an occupancy factor of 0.5 for each pyridinium ring. The pyridinium rings, geometrically approximated as toruses located in the thiourea channels, are not parallel to each other but make an angle of 27°. The cationic dynamics in this intermediate phase can be

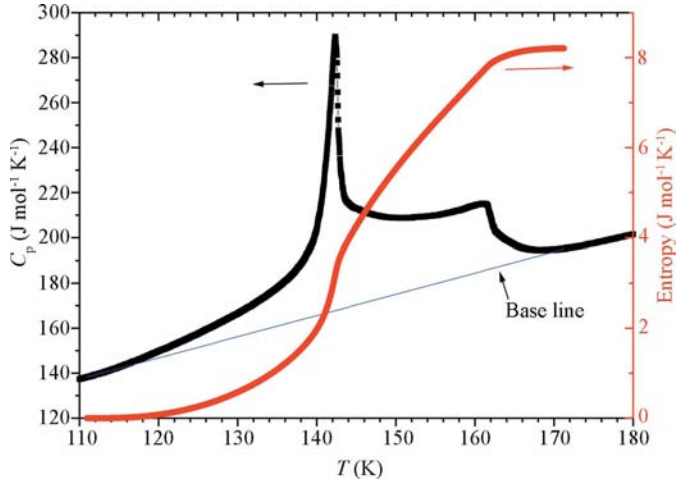

Figure 1
DSC heat capacity measurements (left-hand scale) and calculated entropy changes (right-hand scale).

[1] Supplementary data for this paper are available from the IUCr electronic archives (Reference: WS5061). Services for accessing these data are described at the back of the journal.

described not only by the reorientations around the pseudo C_6 axis perpendicular to the pyridinium ring plane but also by cationic wobbling, which results in constant positional changes of the ring within the thiourea channel. In both high-temperature phases the host thiourea–ionic sublattice is well ordered and there are no significant changes in the geometries of hydrogen bonds between thiourea molecules and between thiourea and the iodide anion.

At 140 K, the crystal undergoes a reversible structural phase transition into the low-temperature orthorhombic phase, space group $P2_1cn$ (standard setting $Pna2_1$, No. 33). The structure of the low-temperature phase determined at 110 K fully confirms the results obtained by Prout *et al.* (2000). The *C*-centring vanishes and the new space group remains noncentrosymmetric. There are two thiourea molecules, one pyridinium ion and one iodide ion in the asymmetric unit. The pyridinium cation is fully ordered with a localized N-atom position. The pyridinium rings located in the channels are not parallel to each other but make an angle of 15.4°. In addition to weak electrostatic interactions (C—H···S,I$^-$) between the pyridinium C atoms and the thiourea S atom and I$^-$ anions, there is one N—H···S hydrogen bond (with an N···S distance of 3.318 Å and an N—H···S angle of 167°), which is strong enough to displace the pyridinium ions from the centre of the channels.

Unlike in the bis(thiourea) pyridinium nitrate salt (Małuszyńska & Czarnecki, 2006), where a ferroelectric phase transition was accompanied by pseudo-merohedral twinning, in the title compound, the iodide derivative, the ferroelectric phase transition at 161 K is accompanied only by merohedral twinning, which is not directly detectable from the X-ray diffraction pattern. The absolute structure *x* value (Flack, 1983) converged to 0.35 (10) in phase II and to 0.46 (7) in phase III. In both phases only ferroelectric domains are present.

The packing arrangement down the *c* axis presented in Fig. 2 shows relatively small positional changes in the thiourea molecules with respect to the thiourea–ionic sublattice in each crystal phase.

3.3. Entropy change of the phase transitions

Phase transitions in crystals can be classified, among others, as displacive or order–disorder type. One of the methods permitting a classification of phase transitions is by determination of the entropy change of transition. If the change in the entropy at the phase transition is above 3 J mol^{-1} K^{-1} it is classified as of the order–disorder type, while if it is below this value the transition is regarded as being of the displacive type. The entropy of a phase transition is determined from measurements of the specific heat over a wide range of temperatures. If the anomalous component of the specific heat related to the phase transitions is separated from the regular specific heat $C_{p0}(T)$, the entropy related to the order–disorder phase transition is

$$\Delta S = \int [C_p(T) - C_{p0}(T)]/T \, dT, \qquad (1)$$

where $C_p(T)$ is the measured specific heat, $C_{p0}(T)$ is the regular component of the specific heat (the base line) and ΔS is the entropy change at the phase transition.

The change in entropy ΔS at the phase transition depends significantly on the choice of the baseline. From our structural studies, the pyridinium cation is strongly disordered in phases

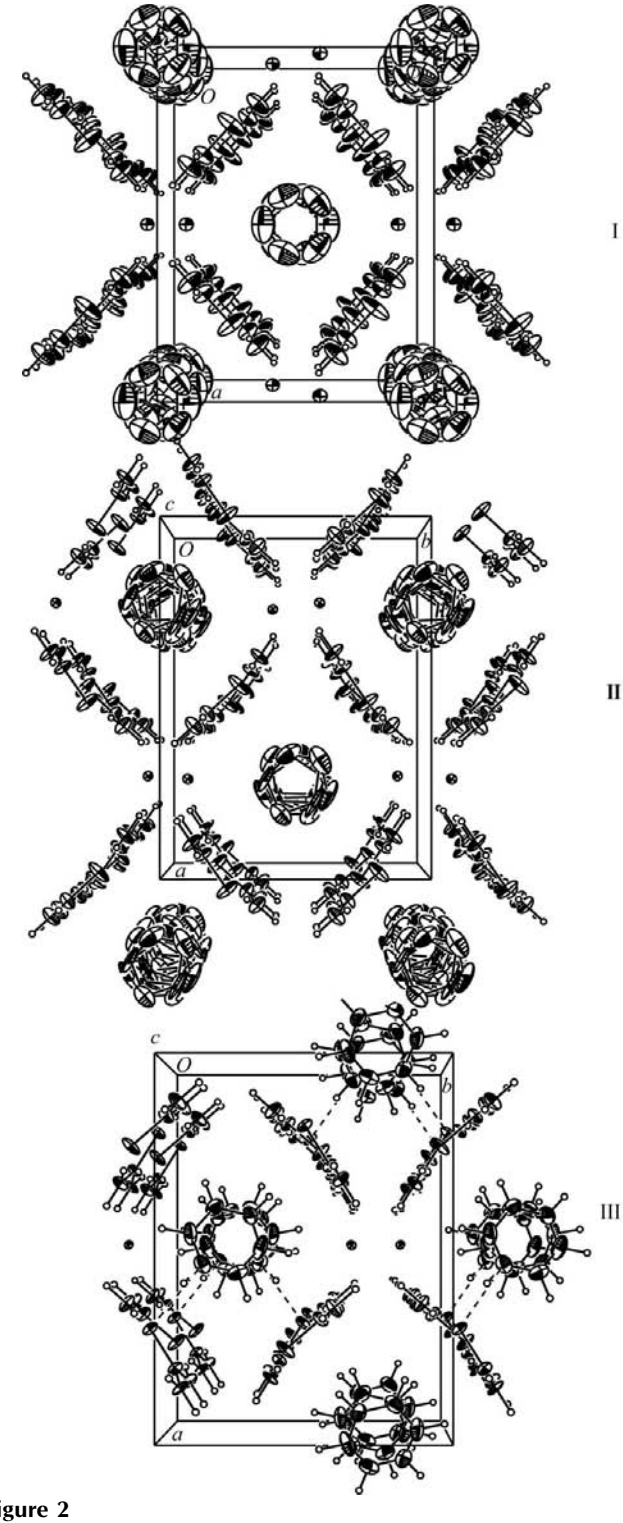

Figure 2
Crystal structures of the three phases of T_2PyI, each viewed along the *c* axis.

I and II. Knowing the changes in entropy accompanying these two phase transitions, it is possible to find the number of distinguishable positions of the cation from

$$\Delta S = R\ln(N_1/N_2), \quad (2)$$

where N_1 and N_2 are the numbers of distinguishable positions of the cation in the disordered and in the ordered phases.

As the crystal studied undergoes two phase transitions, the total change in entropy is the sum of the changes at the two temperatures

$$\Delta S = \Delta S_{T1} + \Delta S_{T2}. \quad (3)$$

The total experimentally found change in entropy at these two phase transitions is close to $\Delta S = 8.2\ \mathrm{J\ mol^{-1}\ K^{-1}}$ (Fig. 1), which indicates that these transitions are of the order–disorder type. The actual change may be a little greater because we had to disregard the long, anomalous tail in the temperature dependence of the specific heat, running to very low temperatures, as the integration in (1) could be performed only for the temperatures accessible to the DSC instrument. One might expect the change in the entropy to be around $R\ln(6)$ ($\sim$15 $\mathrm{J\ mol^{-1}\ K^{-1}}$) because of the disorder of the pyridinium cation. This would be the case when the N atom of the pyridinium ring is equally distributed over six equipotential positions as in pyridinium tetrafluoroborate (Szafraniak *et al.*, 2000). However, the disorder of the cation in T_2PyI is different from this. It is difficult to determine the actual number of distinguishable positions of the cation in phases I and II because of the relatively small difference in the phase transition temperatures T_1 and T_2 and the consequent partial overlapping of the tails of the temperature dependencies of specific heat at the two phase transitions. The entropy change characterizing the transition at T_1 is nearly half of the total entropy change $\Delta S_{T1} = 0.5\,\Delta S$ (about 4.1 $\mathrm{J\ mol^{-1}\ K^{-1}}$), and consequently the entropy change accompanying the transition at T_2 is of similar magnitude, $\Delta S_{T2} = 0.5\,\Delta S$. The values of ΔS_{T1} and ΔS_{T2} are close to the theoretically predicted value of $R\ln(2) = 5.6\ \mathrm{J\ mol^{-1}\ K^{-1}}$ for a model in which, at subsequent phase transitions, the number of distinguishable positions of the cation is reduced by a factor of two, $\Delta S_1 = \Delta S_2 = R\ln(2)$. Given that in the low-temperature ordered phase III the cation is fully ordered and there is one possible position of the cation ($N_2 = 1$), in the disordered phase I there are four distinguishable positions of the cation ($N_1 = 4$), and $\Delta S = R\ln(4)$. The transition from the high-temperature disordered phase I to the low-temperature ordered phase III thus takes place in two stages: at T_1 the number of distinguishable cation positions is reduced from 4 to 2, and at T_2 this number is further reduced to 1. The above conclusions are confirmed by the crystalline structures of all three phases. In the high-temperature phase I the pyridinium ring plane can take two positions as a result of the wobbling, and the other two result from the reorientation about the pseudo-sixfold axis of the ring.

3.4. Dielectric results

Fig. 3 presents the temperature dependence of the real component of permittivity measured at a few frequencies of the measuring field. At T_1 the dependence shows a broad maximum whose presence and shape suggest the ferroelectric character of the transition. The value of permittivity at T_1 is not high, but similar values have been reported for other polycrystalline ferroelectrics from the group of pyridinium salts (Czarnecki *et al.*, 1994*a*). The small anomaly in the temperature dependence of permittivity noted at T_2 has a distinctly different character and is related to a nonferroic transition in which only the translational symmetry changes (the elementary cell is no longer centred). Above 200 K the permittivity increases monotonically (Fig. 3), and the increase is particularly pronounced for low frequencies of the measuring field. This is a consequence of the ionic conductivity of the polycrystalline sample. Similar behaviour has been observed in many pyridinium salts subjected to measurements in the form of polycrystalline samples (Czarnecki *et al.*, 1994*a*).

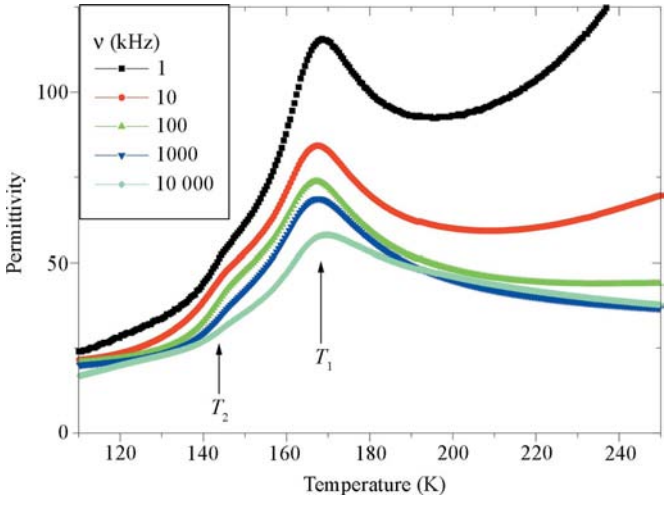

Figure 3
Permittivity dependence on temperature for a selection of frequencies. At T_1 the curves are in the order 1, 10, 10^2, 10^3, 10^4 kHz.

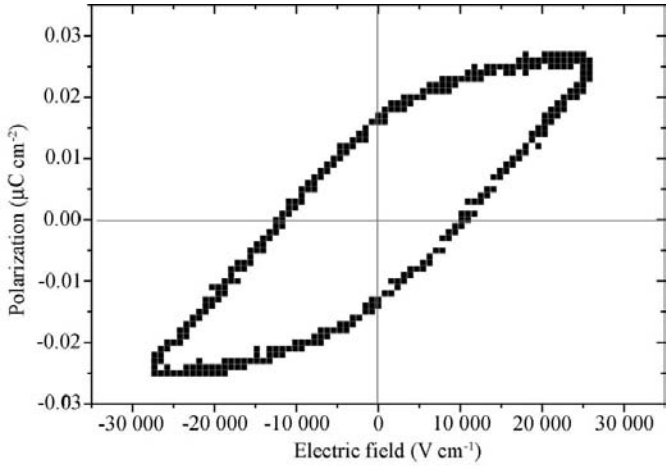

Figure 4
Dielectric hysteresis loop at 157 K.

Direct evidence of ferroelectric properties of a given material is given by the electric hysteresis loop. In polycrystalline materials it is often difficult to observe the hysteresis loop (Małuszyńska & Czarnecki, 2006; Czarnecki *et al.*, 1994*a*,*b*), but in T_2PyI we observed hysteresis loops (Fig. 4) at 157 K, a few degrees below the Curie point at T_1. At temperatures much lower than the Curie point it was impossible to observe the hysteresis loop because of a rapid increase in the coercive field. Spontaneous polarization in the polycrystalline sample of the compound studied was only of the order of 0.01 μC cm^{-2}, but similar values have been observed in polycrystalline samples of ferroelectric pyridinium salts (Czarnecki *et al.*, 1994*a*,*b*). The change in the crystal symmetry at the Curie point at T_1 (*Cmcm* $\rightarrow$ *C*2*cm*) implies that the new ferroelectric phase belongs to the uniaxial type. This phase transition is ferroelectric but not ferroelastic, because both phases are in the orthorhombic system and we may expect only ferroelectric but not ferroelastic domains in low-temperature phases.

The ferroelectricity of T_2PyI is most probably related to the ordering of the pyridinium cation, which possesses a dipole moment. In the high-temperature phase, the average dipole moment is zero because of the pyridinium cation reorientation, which is consistent with the results of structural studies indicating that the pyridinium cation is at the centrosymmetric 2/*m* site. Below T_1 the symmetry plane disappears and the average dipole moment of all cations of the elementary cell has a component that is different from zero along the *x* axis, which becomes the ferroelectric axis. Although the phase transition at T_1 is of the order–disorder type, the ferroelectric phase below T_1 should be still treated as disordered, as the pyridine cation still performs reorientations. The difference is that in this phase the reorientations do not lead to a zero average value of the dipole moment. The low-temperature phase III is ordered and, like phase II, is ferroelectric, but the high value of the coercive field prevents the observation of the hysteresis loop. The value of spontaneous polarization obtained from measurements of the hysteresis loop on a polycrystalline sample cannot be compared with the calculated value. We expect that the main contribution to spontaneous polarization is from the dipole moment of the pyridinium cation. Assuming the dipole moment is about 1.88 D (Beck *et al.*, 2003), the rough estimate of spontaneous polarization at low temperatures is about 1.6 μC cm^{-2}. At the phase transitions the shape of the walls of the square cross-sectional channel formed by the thiourea molecules changes. In the high-temperature phase I the walls are planar, while in the ferroelectric phase II and the ordered phase III they are curved (Fig. 1). The reason for this change is that the gradual ordering of the cation takes place as a result of the formation of hydrogen bonds between the N atom of the pyridinium cation and the S atom of the thiourea molecule. Although, these hydrogen bonds are weak, as judged by the N$\cdots$S distance, their formation is most probably the cause of the phase transitions in T_2PyI.

4. Conclusions

We draw the following conclusions:

(1) T_2PyI has been found to undergo two, not one, phase transitions (Prout *et al.*, 2000): a continuous phase transition at T_1 = 161 K and a discontinuous but close to continuous one at T_2 = 141 K, corresponding to the following symmetry changes: *Cmcm* (I) $\rightarrow$ *C*2*cm* (II) $\rightarrow$ $P2_1cn$ (III).

(2) The entropy changes accompanying the phase transitions indicate that they are both of the order–disorder type.

(3) The high-temperature phase I and the intermediate phase II are disordered, with the pyridinium cation free to perform in-plane and out-of-plane reorientations.

(4) In all three phases the T_2PyI structure can be approximately described as having relatively rigid channels formed by the thiourea (host) molecules, with the pyridinium (guest) cations localized inside the channels.

(5) The ordering of the pyridinium cation at subsequent phase transitions is related to the formation of weak hydrogen bonds between the N atom of the cation and the S atom of the thiourea molecule.

(6) The phase transitions lead to the ordering of pyridinium cations, inducing a small curvature of the channel walls formed by thiourea molecules.

(7) Phase II and phase III of the T_2PyI crystals are ferroelectric and nonferroelastic; this new ferroelectric belongs to the uniaxial order–disorder type of ferroelectrics.

This work was partially financed by the Ministry of Science and Higher Education from 2006–2008 funds, grant No. N202 134 31/2331.

References

Beck, B., Villanueva-Garibay, J., Muller, K. & Roduner, E. (2003). *Chem. Mater.* **15**, 1739–1748.
Czarnecki, P., Nawrocik, W., Pająk, Z. & Wąsicki, J. (1994*a*). *J. Phys. Condens. Matter*, **6**, 4955–4960.
Czarnecki, P., Nawrocik, W., Pająk, Z. & Wąsicki, J. (1994*b*). *Phys. Rev. B*, **49**, 1511–1512.
Flack, H. D. (1983). *Acta Cryst.* A**39**, 876–881.
Harris, K. D. M. (1996). *J. Mol. Struct.* **374**, 241–250.
Hollingsworth, M. D. & Harris, K. D. M. (1996). *Comprehensive Supramolecular Chemistry*, Vol. 6, pp. 177–237. New York: Pergamon.
Kuma Diffraction (1999). *KM*-4 *Software*. Kuma Diffraction, Wrocław, Poland.
Małuszyńska, H. & Czarnecki, P. (2006). *Z. Kristallogr.* **221**, 218–225.
Pająk, Z., Czarnecki, P., Małuszyńska, H., Szafrańska, B. & Szafran, M. (2000). *J. Chem. Phys.* **113**, 848–853.
Pająk, Z., Czarnecki, P., Wąsicki, J. & Nawrocik, W. (1998). *J. Chem. Phys.* **109**, 6420–6423.
Pająk, Z., Małuszyńska, H., Szafrańska, B. & Czarnecki, P. (2002). *J. Chem. Phys.* **117**, 5303–5310.
Prout, K., Heyes, S. J., Dobson, Ch. M., McDaid, A., Maris, T., Mueller, M. & Seaman, M. J. (2000). *Chem. Mater.* **12**, 3561–3569.
Scott, J. F. (2000). *Ferroelectric Memories 2000.* Berlin: Springer.
Sheldrick, G. M. (2008). *Acta Cryst.* A**64**, 112–122.
Szafraniak, I., Czarnecki, P. & Mayr, P. U. (2000). *J. Phys. Condens. Matter*, **12**, 643–652.
Truter, M. R. & Vickery, B. L. (1972). *Acta Cryst.* B**28**, 387–393.
Wąsicki, J., Czarnecki, P., Pająk, Z., Nawrocik, W. & Szczepański, W. (1997). *J. Chem. Phys.* **107**, 576–579.